MEMORANDUM REPORT BRL-MR-3852

BRL

PREDICTION OF IN-BORE AND AERODYNAMIC HEATING OF KE PROJECTILE FINS

WALTER B. STUREK
HARRY A. DWYER
EARL N. FERRY, JR.

AUGUST 1990

U.S. ARMY LABORATORY COMMAND

BALLISTIC RESEARCH LABORATORY
ABERDEEN PROVING GROUND, MARYLAND

NOTICES

Destroy this report when it is no longer needed. DO NOT return it to the originator.

Additional copies of this report may be obtained from the National Technical Information Service, U.S. Department of Commerce, 5285 Port Royal Road, Springfield, VA 22161.

The findings of this report are not to be construed as an official Department of the Army position, unless so designated by other authorized documents.

The use of trade names or manufacturers' names in this report does not constitute indorsement of any commercial product.

REPORT DOCUMENTATION PAGE

Form Approved
OMB No. 0704-0188

1. AGENCY USE ONLY (Leave blank)	2. REPORT DATE	3. REPORT TYPE AND DATES COVERED
	August 1990	Final, Jun 88 - Aug 89

4. TITLE AND SUBTITLE
Prediction of In-bore and Aerodynamic Heating of KE Projectile Fins

5. FUNDING NUMBERS
PR: 1L162618AH80
62618A-00-001 AJ

6. AUTHOR(S)
Walter B. Sturek, Harry A. Dwyer*, and
Earl N. Ferry, Jr.

7. PERFORMING ORGANIZATION NAME(S) AND ADDRESS(ES)

8. PERFORMING ORGANIZATION REPORT NUMBER

9. SPONSORING / MONITORING AGENCY NAME(S) AND ADDRESS(ES)
U.S. Army Ballistic Research Laboratory
ATTN: SLCBR-DD-T
Aberdeen Proving Ground, MD 21005-5066

10. SPONSORING / MONITORING AGENCY REPORT NUMBER
BRL-MR-3852

11. SUPPLEMENTARY NOTES
* University of California, Davis
Department of Mechanical Engineering, College of Engineering
Davis, CA 95616

12a. DISTRIBUTION / AVAILABILITY STATEMENT
Approved for public release; distribution unlimited

12b. DISTRIBUTION CODE

13. ABSTRACT (Maximum 200 words)

Current high velocity kinetic energy penetrator shell use fins made of aluminum to provide aerodynamic stability. Due to the high velocity of the shell and the requirement to keep the drag of the shell to a minimum, these aluminum fins are very thin, a maximum thickness of 4 mm is typical. The thin cross section of the fin and the low melting point of aluminum combine to create a critical design problem. If the fins do no have sufficient mass to absorb and conduct away the high heat loads imposed in-bore and in-flight, the fins will ablate and cause erratic flight due to distortion of the fin or the lack of sufficient fin area to maintain stability. This report discusses the development of an improved predictive capability to model the unsteady heat conduction of fin configurations of interest to the Army. Two modeling capabilities are described: (1) the full three-dimensional geometry of the fin for a fixed geometry; and (2) a quasi-three dimensional, two-phase modeling of the fin in which melting of the fin is simulated with a moving boundary that recedes as the material reaches melt temperature. Sample computations are shown which illustrate the unsteady, thermal response of KE projectile fins to aerodynamic heating.

14. SUBJECT TERMS	15. NUMBER OF PAGES
Aerodynamic Heating; KE Projectiles; Unsteady Heat Conduction Fins; Finned Projectile	51
	16. PRICE CODE

17. SECURITY CLASSIFICATION OF REPORT	18. SECURITY CLASSIFICATION OF THIS PAGE	19. SECURITY CLASSIFICATION OF ABSTRACT	20. LIMITATION OF ABSTRACT
UNCLASSIFIED	UNCLASSIFIED	UNCLASSIFIED	UL

INTENTIONALLY LEFT BLANK.

Table of Contents

		Page
	List of Figures	v
I.	INTRODUCTION	1
II.	PROBLEM DEFINITION AND BASIC EQUATIONS	1
	1. BOUNDARY CONDITIONS AND INPUT PARAMETERS	5
	2. NUMERICAL METHOD	5
III.	RESULTS	6
	1. QUASI-3D MELTING FIN	6
	2. FULL 3D FIN WITHOUT MELTING - IN-BORE HEAT TRANSFER	7
	3. FULL 3D FIN WITHOUT MELTING - AERODYNAMIC HEATING	8
IV.	CONCLUDING REMARKS	8
	References	19
	List of Symbols	21
	APPENDIX A: CODE IMPLEMENTATION ON THE BRL CRAY2	23

INTENTIONALLY LEFT BLANK.

List of Figures

Figure		Page
1	Schematic drawing of generic KE projectile	9
2	Schematic drawing of KE projectile fin	10
3	Illustration of interpolation scheme to transfer geometry and physical properties from a Cartesian system to the computational grid	11
4	Quasi-3D melting fin, Time = 1.0 second	12
5	Quasi-3D melting fin, Time = 2.0 seconds	13
6	Quasi-3D melting fin, Time = 3.0 seconds	14
7	Full 3D fin modeling, Time = 1.0 second	15
8	Full 3D fin modeling, Time = 2.0 seconds	16
9	Full 3D fin modeling, Time = 3.0 seconds	17

INTENTIONALLY LEFT BLANK.

I. INTRODUCTION

Current high velocity kinetic energy penetrator shell use fins made of aluminum to provide aerodynamic stability. In order to provide some protection to the aluminum fins, a 0.08 to 0.15 mm coating of aluminum oxide is applied. Due to the high velocity of the shell and the requirement to keep the drag of the shell to a minimum, the aluminum fins are very thin, a maximum thickness of 3 to 5 mm is typical. The thin cross-section of the fin and the low melting point of aluminum combine to create a critical design problem. If the fins do not have sufficient mass to absorb and conduct away the high heat loads imposed in-bore and in-flight, the fins will ablate and cause erratic flight due to distortion of the fin or the lack of sufficient fin area to maintain stability.

The Computational Aerodynamics Branch of the US Army Ballistic Research Laboratory (BRL), Aberdeen Proving Ground, Maryland, has been involved in providing computational predictions for the unsteady thermal response of fins to designers of KE projectiles.[1] Previous predictive capabilities were limited to planar, single-phase, two-dimensional modeling. The purpose of this report is to discuss the development of an improved predictive capability which includes the ability to model the full three-dimensional geometry of the fin for a fixed geometry and a quasi-three dimensional, two-phase modeling of the fin in which melting of the fin is simulated with a moving boundary that receeds as the material reaches the temperature of melt.

The development of this predictive capability is described and sample computations are shown which illustrate the unsteady, thermal response of KE projectile fins to aerodynamic heating. The computations have been carried out using the Cray 2 computer located at the BRL.

II. PROBLEM DEFINITION AND BASIC EQUATIONS

The basic geometry of a generic KE projectile and fins is shown in Figure 1. The features of the fin geometry are: (1) the leading edge sweep which reduces the maximum heat transfer coefficient at the leading edge; (2) the fin span; (3) the variable chord length from the root to the tip; and (4) the very thin thickness of the fin which includes a taper from the root to the tip. These fins are predominately made of high strength aluminum. Since aluminum has a high thermal conductivity and relatively low melting point (950 K), a thin coating of aluminum oxide is applied which has been found to be very effective in retarding erosion effects which are a result of exposure to the gun gases and the subsequent aerodynamic heating.

The basic physical processes which occur near the fin surface are associated with the viscous boundary-layer, protective coating, and the solid fin material. It has been assumed in the present study that the thin protective coating is in a quasi-steady condition and that the major influence of the coating is to offer a resistance to heat transfer from the boundary layer. This same assumption of the lack of unsteady influences is also made in the boundary layer and is felt to be equally appropriate for the aluminum oxide coating.

With the aerodynamic boundary-layer and the aluminum oxide coating both treated with a quasi-steady assumption and neglecting effects due to melting, the heat transfer per unit area into the interior of the fin is given by the following formula, which results from considering the conservation of energy.

$$q_{bl} = q_f = q_{sur} = (T_o - T_s) \Big/ \left(\frac{1}{h_{bl}} + \frac{\Delta x_f}{k_f} \right) \tag{1}$$

where the following notation has been employed.

q_{bl} = heat flux through viscous boundary-layer

q_f = heat flux through coating

q_{sur} = heat flux at surface of fin

T_o = local adiabatic wall temperature

T_s = surface temperature of the aluminum

h_{bl} = local boundary-layer convective heat transfer coefficient

Δx_f = local thickness of the alumina coating

k_f = thermal conductivity of the alumina coating.

The above equation serves as a boundary condition for the surface control volume. The surface temperature, T_s, is one of the unknowns of the system of equations, and is calculated during the history of the projectile flight.

The basic law which is utilized to calculate the thermal history of the fin is the control volume form of the first law of thermodynamics applied to a solid body. The form shown below involves grid velocities and time-dependent volumes.

Energy Equation

$$\frac{\partial}{\partial_t} \left[\int \int \int \rho e dV \right] = - \left[\int \int \rho e \vec{V}_b \bullet d\vec{A} \right] - \int \int \vec{q} \bullet d\vec{A} \tag{2}$$

where the following notation is used.

ρ = density

e = internal energy = $c_v T$

$\vec{q}$ = conduction heat flux = $-k \nabla T$, outward direction positive

V = volume

$\vec{V}_b$ = velocities of the grid boundaries, $\vec{V}_b$, positive outward

$\vec{A}$ = local surface area

T = temperature

c_v = specific heat.

If the control volumes are moving in space and time due to melting, the outer boundary velocity, $\vec{V}_b$, is determined using Equation (3). This relation follows from a heat balance considering the heat transferred into the control volume at the outer surface, the heat absorbed in melting of the material, and the heat transferred to adjacent volume segments.

$$h_{ml}\,(T_o - T_{melt}) = -\rho L_h \vec{V}_b \bullet \vec{n} - \vec{q}_{adj} \bullet \vec{n} \tag{3}$$

where

h_{ml} = local boundary-layer convective heat transfer coefficient for melting surface $h_{ml} = h_{bl}$ is assumed in this study

T_{melt} = melt temperature of the fin

L_h = latent heat of the melting fin material

$\vec{n}$ = unit normal vector

$\vec{q}_{adj}$ = heat transfer per unit area to adjacent control volumes.

It is best to rewrite Equation (2) in a dimensionless form in order for the physical scaling in space and time to be normalized. The dimensionless form (constant properties) of the moving control volume energy equation after substituting $\vec{q} = -k\nabla T$ is:

Dimensionless Form of the Energy Equation

$$\frac{\partial}{\partial_\tau}\left[\int\int\int T' dV'\right] = -\int\int T'\vec{V}_b' \bullet d\vec{A}' + \int\int \nabla T' \bullet d\vec{A}' \tag{4}$$

where all volumes and areas have been made dimensionless with the characteristic length, L, and the following definitions have been used.

$$\alpha = \frac{k}{\rho c_v}$$

$$\tau = \frac{t\alpha}{L^2}$$

$$T' = \frac{T}{T_{ref}}$$

$$\vec{V}_b' = \frac{\vec{V}_b L}{\alpha}$$

$$\vec{A}' = \frac{\vec{A}}{L^2}$$

$$V' = \frac{V}{L^3}$$

The final approximation that was employed in the present study was to assume that the temperature gradients across the fin thickness were very small relative to the temperature gradients between the fin and the projectile body (this is the classical "thin fin" approximation of heat transfer). For aerodynamic heating of fins on supersonic projectiles, this seems to be a very good approximation since their thickness to length or width ratio is usually of the order of 1/10th to 1/100th. This approximation will be checked out using a full three dimensional modeling of the fin which is described later in this report.

The neglect of the temperature gradients across the thickness of the fin allows for the control volume equations to be averaged in the thickness or z- direction, and the problem is reduced to two space variables for the energy equation. However, the three-dimensional aspect of the physics is retained in the problem through the volume of the cells which varies in the z-direction as a function of the distance away from the body surface (y-direction). Since real aerodynamic fins do have substantial variations of thickness, it is important to include this effect in the analysis. The major thermal effects of the varying thickness are to increase the thermal inertia of the cells and to increase the area for heat transfer into the projectile body.

Also, since the calculations which include effects of melting have a moving grid, new computational grids have to be generated at each time step as well as new areas and volumes for the control volumes.

A typical or generic fin used on a supersonic projectile is shown in Figure 2. The figure shows the $x - y$ plane where the temperature gradients exist. The z-thickness is perpendicular to the $x - y$ plane. For the results presented in this section of the paper, the fin dimensions are as indicated in Figure 2.

1. BOUNDARY CONDITIONS AND INPUT PARAMETERS

Local values for the heat transfer coefficient and adiabatic wall temperature are required as boundary conditions for the heat conduction solutions. Values for these parameters are obtained using PLNRASCC[2] as an auxiliary computer program. These quantities are determined as a function of the geometry of the fin and the velocity history of the projectile. Since one objective of the development of the predictive capability is to provide a design tool for projectile designers, the input to the program has been organized to require a minimum of parameters. This has been accomplished as illustrated in Figure 2 and Figure 3 where the computational grid, is used to define the basic fin geometry, is shown overlayed on a regular cartesian grid. This allows the fin geometry to be specified using a minimum of parameters familiar to the projectile designer. The computer code input routine performs an appropriate interpolation to assign properties to the computational grid without operator intervention.

In order to input the convective heat transfer coefficient data in this initial code development, a simplified procedure was implemented. The procedure uses a cosine function to define the variation of h_{bl} from the fin leading edge to the trailing edge. The function used is shown below at Equation (5) where

h_{max} = h_{bl} at the fin leading edge

h_{min} = h_{bl} on the fin flat surface

Δc = increment along fin chord where the value of h_{bl} changes from h_{max} to h_{min}

x_{loc} = distance from fin leading edge

h_{loc} = local value of h_{bl}

$$h_{loc} = h_{min} + \frac{1}{2}(h_{max} - h_{min})\left\{cos\left[\left(\frac{x_{loc}}{\Delta c}\right)\pi\right] + 1\right\} \tag{5}$$

Values of h_{max} and h_{min} used in this initial study were 6000 and 1500 $J/kg - m^2$, respectively, which are representative for the M735 projectile at launch velocity.

When x_{loc} becomes greater than Δc, the value of h_{loc} is set to h_{min}. This procedure preserves the correct variation of h_{bl} from the fin leading edge to the trailing edge with a minimum of required input data.

2. NUMERICAL METHOD

The basic numerical method that was employed to solve the energy equation for the melting fin problem was the predictor/corrector method that was developed by Dwyer.[3] This method has increased stability characteristics over approximate factorization schemes

for skewed and stretched grids with strong diffusion influences. The method has been found to work very well for the present problem, and time steps can be taken which are much larger than the times for physical processes to occur. For the present problems, the time step was decreased until the solution converged in time.

The melting of the fin caused the computer code to be considerably modified in order to account for interface melting and the changing shape of the fin. The criterion used for melting consisted of monitoring the surface temperature until the aluminum melt temperature was reached. After the melting temperature was reached, all of the excess heat transfer was determined by the differences between the total heat fluxes into the control volume. This excess heat flux, which would result in an increase in the bulk temperature of the control volume for a temperature less than t_{melt}, is used to define a change in size of the control volume. This change in volume results from a balance between the excess heat flux and the heat absorbed by the melting material determined using the latent heat of fusion.

With the geometrical normal regression rate of the fin leading edge and top surface determined, the coordinates were changed by shortening the length of the coordinate lines coming from the origin of the grid system (triangular shaped cells were used at the origin to avoid problems with tridiagonal solvers). During a given time step, the entire grid changed by a small amount due to surface melting, and the difference between the old and the new grid locations determined the grid velocity, $\vec{V}_b$. Since the grid used in this problem is nonorthogonal, the geometrically normal regression rate of the surface had to be interpolated onto the grid lines, and this procedure may have the potential for serious errors if the grid becomes highly skewed at the interface. Improvements in this procedure should be investigated in the future.

The grid velocity terms in the control volume equations have a nature which is identical with convection. If the grid velocity does become too high, then Peclet number effects are possible. However, due to the large latent heat of melting of aluminum, the grid velocities are not large.

III. RESULTS

The results will be discussed in three sections to illustrate sample computations for: (1) quasi-3D melting fin; (2) full 3D fin modeling for in-bore heating effects; and (3) full 3D fin without melting for aerodynamic heating alone. The physical properties of the aluminum fin and the aluminum oxide coating are given in Table 1.

1. QUASI-3D MELTING FIN

The results for a typical melting fin solution are shown in Figures 4 through 6 where both the computational grid and isotherm distributions are given at various times for a simulated flight of the projectile. The computational grid was 81×81 nodes; however only a portion of the nodes are shown for clarity. For these calculations, the temperature at

the root of the fin is fixed at the ambient temperature of 293 K which simulates the large thermal inertia of the projectile body. At the trailing edge of the fin an adiabatic condition was employed, which is a reasonable representation of the separated flow in the fin wake. The earliest time result, shown in Figure 4, indicates that melting has not yet occurred, but that the surface temperature of a small portion of the fin near the fin tip has reached the melting temperature of 950 K. An early stage of melting is shown in Figure 5. More advanced melting is shown in Figure 6. As expected, melting starts at the leading edge and the tip of the fin where the thickness of the fin is smallest. The cold wall boundary condition at the root and the increased thickness of the root of the fin combine to retard the temperature rise in that location of the fin.

The results shown in Figure 6 indicate severe regression of the fin span. This result is expected and is confirmed by experimental firing tests (Reference 5). No comparison with experimental data has been shown here since the results are for a generic fin shape. However, the results do compare favorably with previous results (Reference 1).

The 'kinks' in the temperature contours near the trailing edge of the fin which are apparent in Figures 4-6 and to a lesser degree in Figures 7-9 are a result of the grid configuration. The sharp change in direction of the grid lines results in a discontinuity in the variation of the grid metrics. This discontinuity can be controlled by modified grid generation procedures which will be implemented in the future. However, there is no indication that the accuracy of the predicted results is significantly affected.

2. FULL 3D FIN WITHOUT MELTING - IN-BORE HEAT TRANSFER

The projectile is resident for about 13 milliseconds in the gun tube, exposed to the gun propellant gases, before the free flight phase of the trajectory is reached. During this time the fins are exposed to the flame temperature of the propellant which, for standard propellants, is about 3000 K. Using the propellant flame temperature and a convective heat transfer coefficient that has been used in previous studies for in-bore heat transfer (Reference 1), the full 3D code has been used to estimate the thermal response of the fin to the in-bore environment. The results indicate that the surface temperature of the fin reaches a temperature of 350 K at exit of the gun tube. The full indepth temperature

Table 1. Physical Properties.

Property	*Units*	*Aluminum*	*Al_2O_3 Coating*
Thermal Conductivity	w/m-K	193.0	10.0
Density	kg/m^3	2800.0	
Specific Heat, C_v	J/kg - K	869.0	
Latent Heat	J/kg	4.5188×10^4	
Coating Thickness	m		0.00015
T_{melt}	K	950.0	

distribution can then be used as the starting temperature distribution for the aerodynamic heating computations.

3. FULL 3D FIN WITHOUT MELTING - AERODYNAMIC HEATING

A full 3D version of the code has been developed to model the complete geometry of the fin as shown in Figure 2. The computational grid contains 41 × 41 × 9 grid nodes. Sample results are shown in Figures 7, 8 and 9 for different times in the simulated flight. The temperature contour plots show that a region develops starting at the tip and leading edge of the fin in which the temperature has reached melting. The melting region is seen to develop in time in a similar manner as the previous solution which included the moving grid routines. Temperature profiles across the fin thickness indicate only small variation of temperature and confirm the validity of the quasi-3D model for initial design studies. However, in order to eliminate uncertainties as much as possible, the full 3D model of the fin response is recommended.

IV. CONCLUDING REMARKS

This report has described the development of a new computational modeling capability for the unsteady thermal response of KE projectile fins to combined effects of in-bore and free-flight aerodynamic heating. The modeling capability includes the full 3D geometry of the fin for a fixed geometry and a quasi-3D modeling of the fin in which the melting and subsequent ablation of the fin is modeled. These capabilities represent significant enhancement of the previous modeling in which the fin was modeled as a planar two-dimensional shape for a single phase solid material.

In developing the computational technique, particular attention has been given to provide a stable, robust, algorithm along with simplified input characteristics which are familiar to projectile design engineers.

Additional testing of the computational technique for actual fielded projectile designs is required to confirm the validity and usefullness of the code. However, the initial results and operational experience with the code are encouraging.

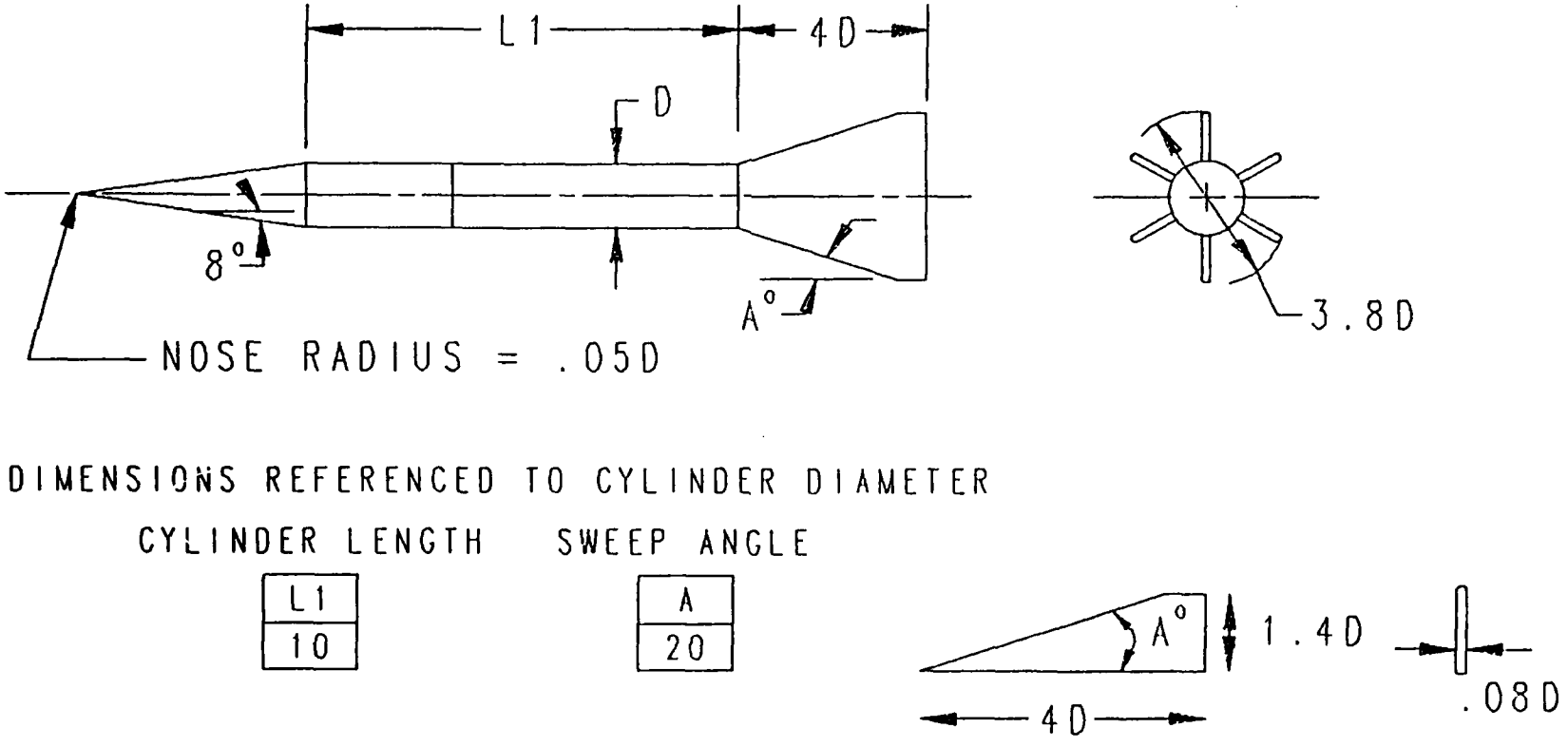

Figure 1. Schematic drawing of generic KE projectile

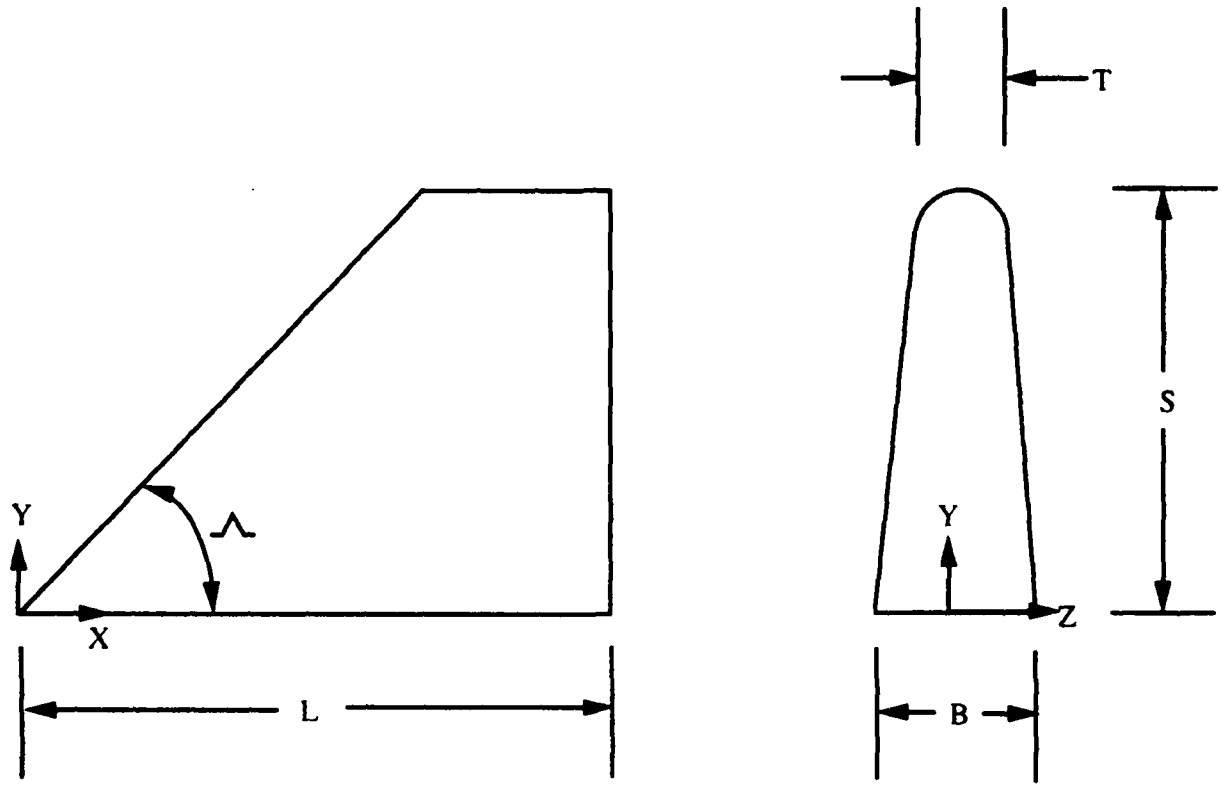

DIMENSIONS IN METERS

NOT TO SCALE

L = 0.090
B = 0.0035
T = 0.0019
S = 0.030
Λ = 20

Figure 2. Schematic drawing of KE projectile fin

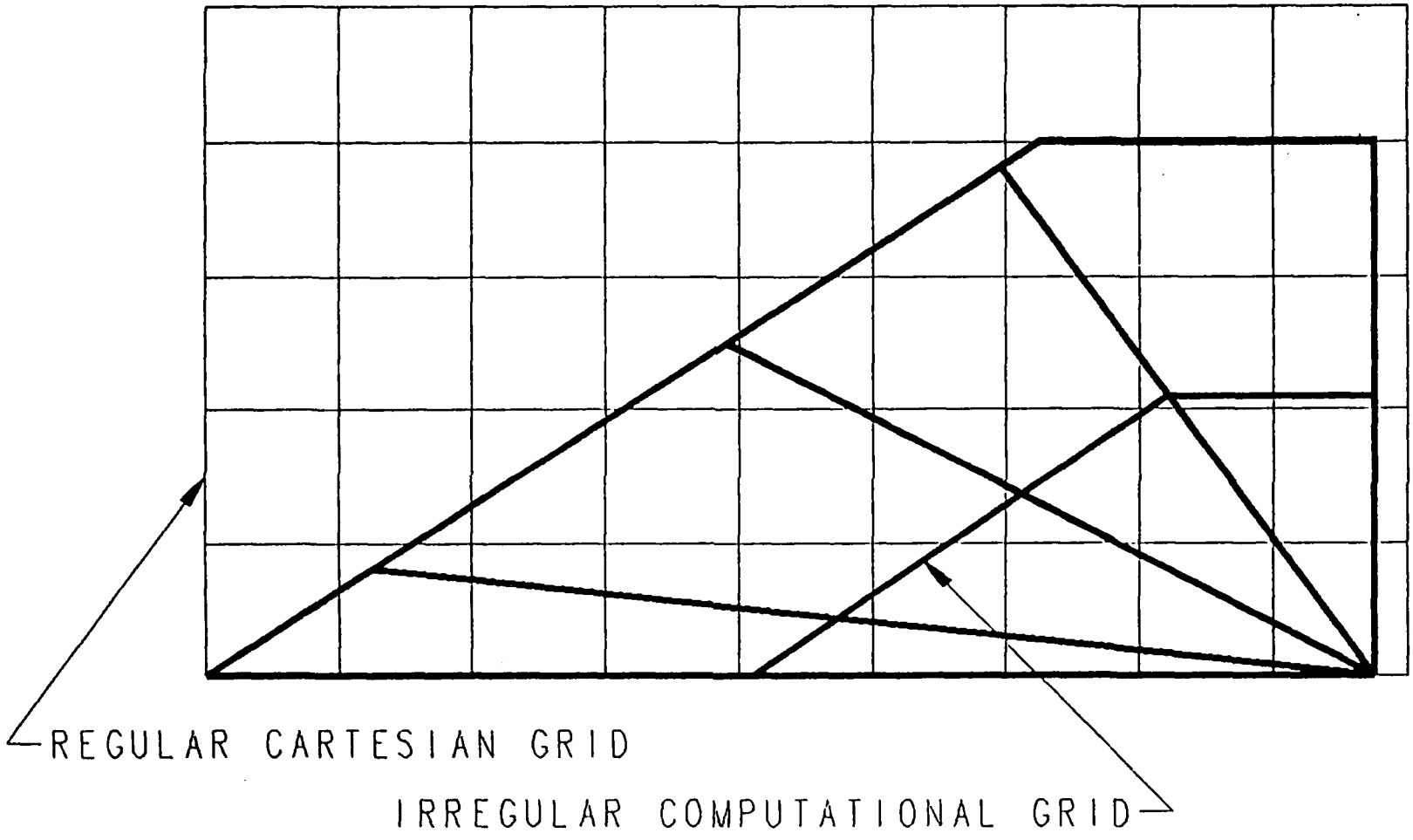

Figure 3. Illustration of interpolation scheme to transfer geometry and physical properties from a Cartesian system to the computational grid

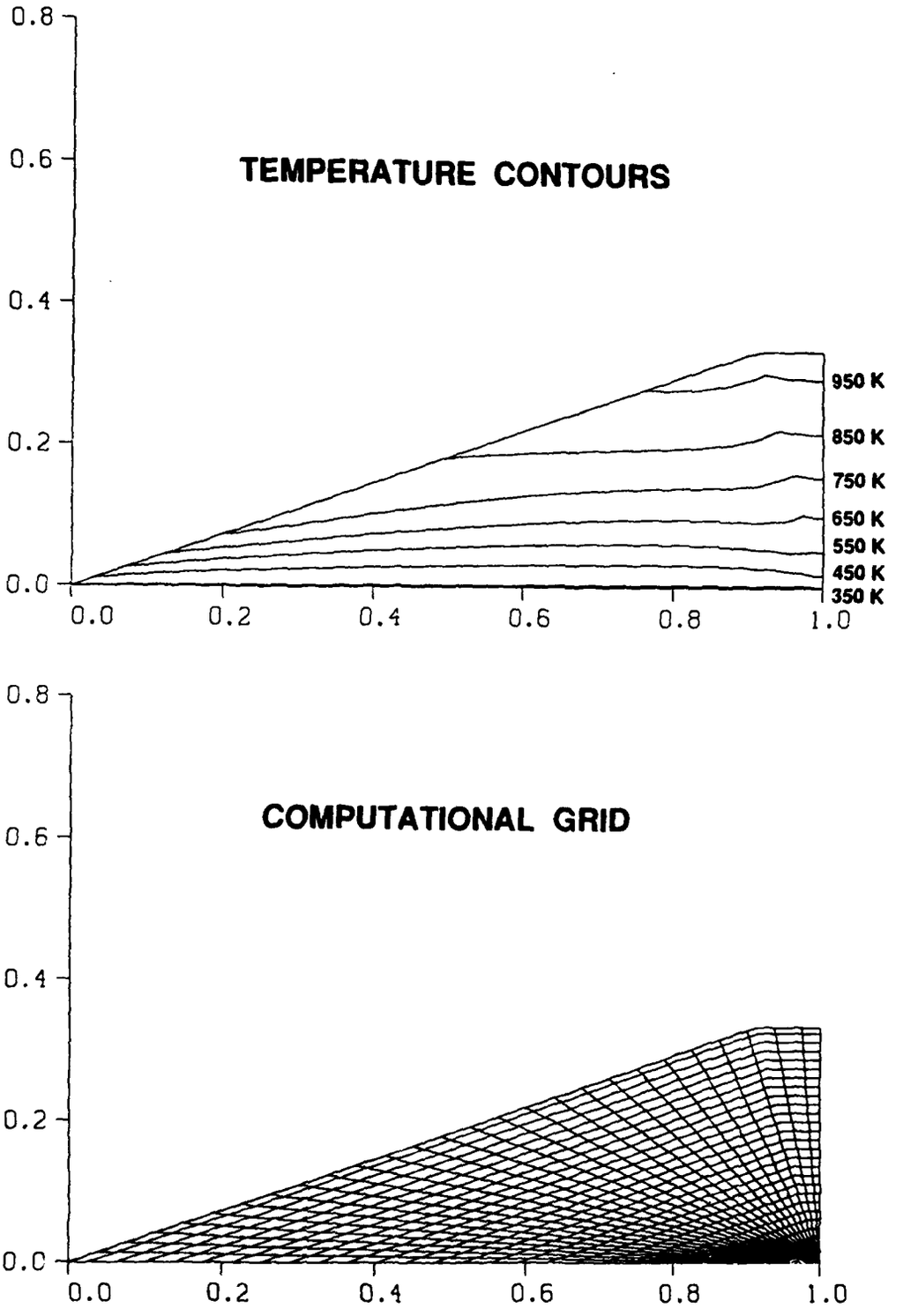

Figure 4. Quasi-3D melting fin, Time = 1.0 second

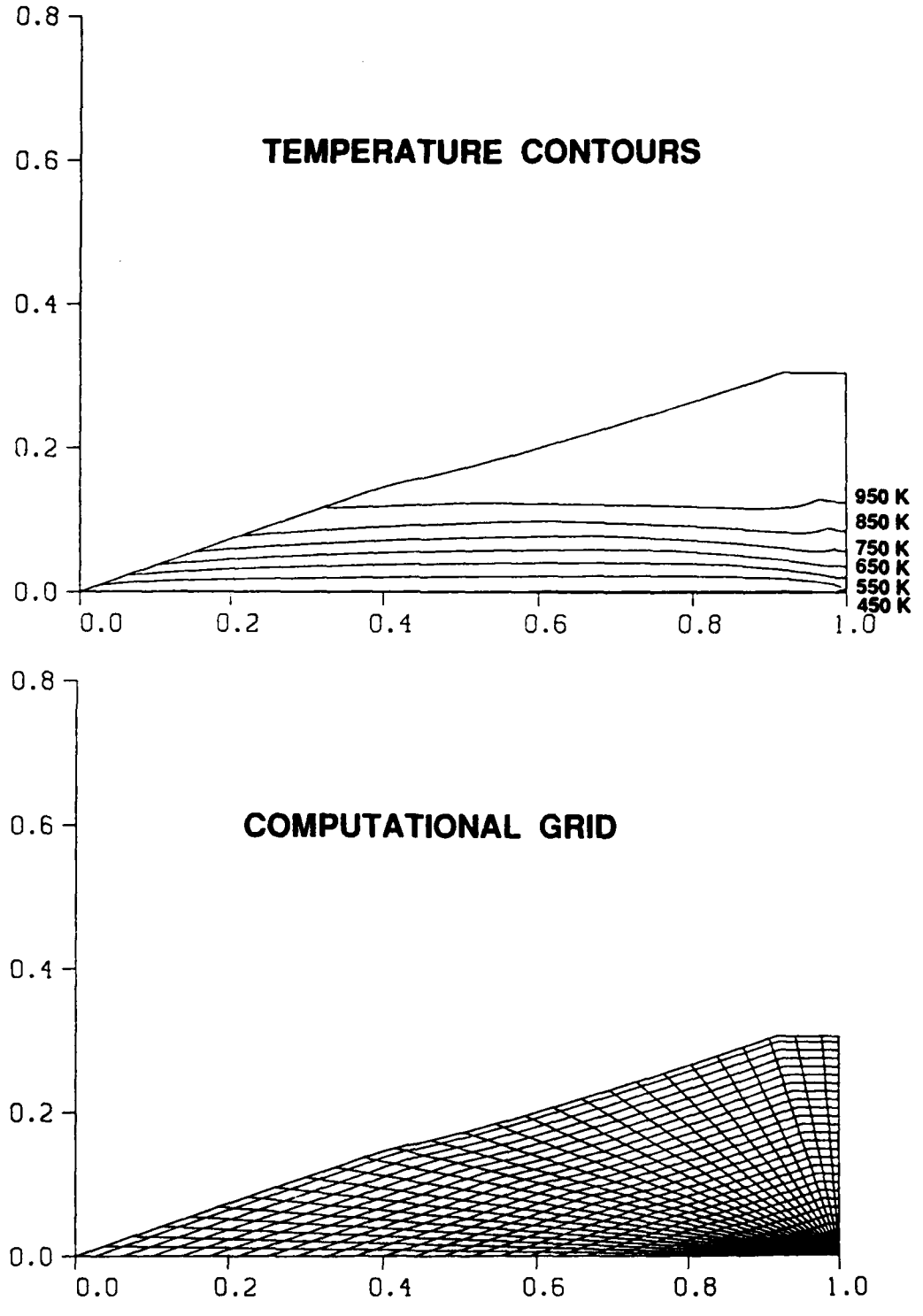

Figure 5. Quasi-3D melting fin, Time = 2.0 seconds

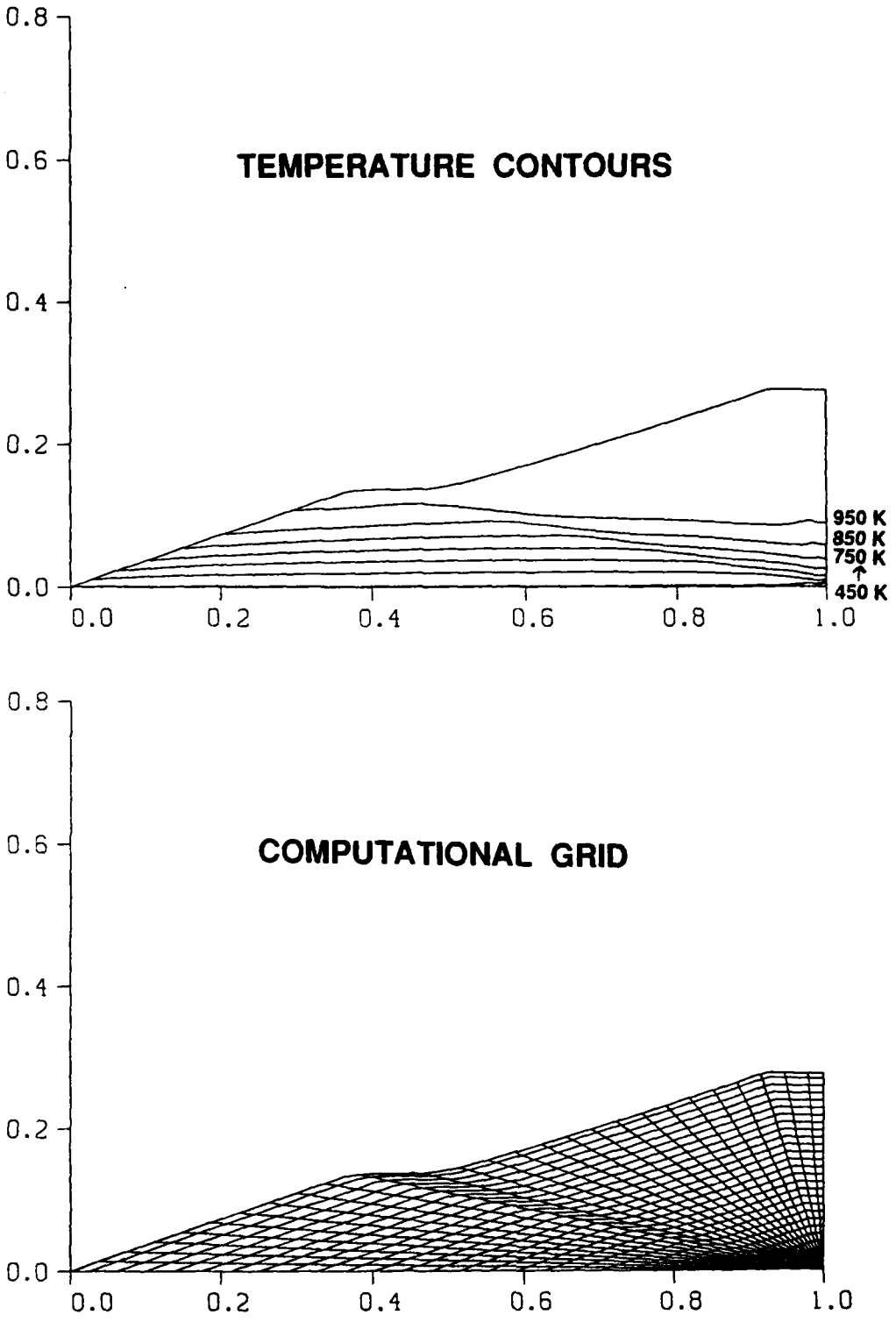

Figure 6. Quasi-3D melting fin, Time = 3.0 seconds

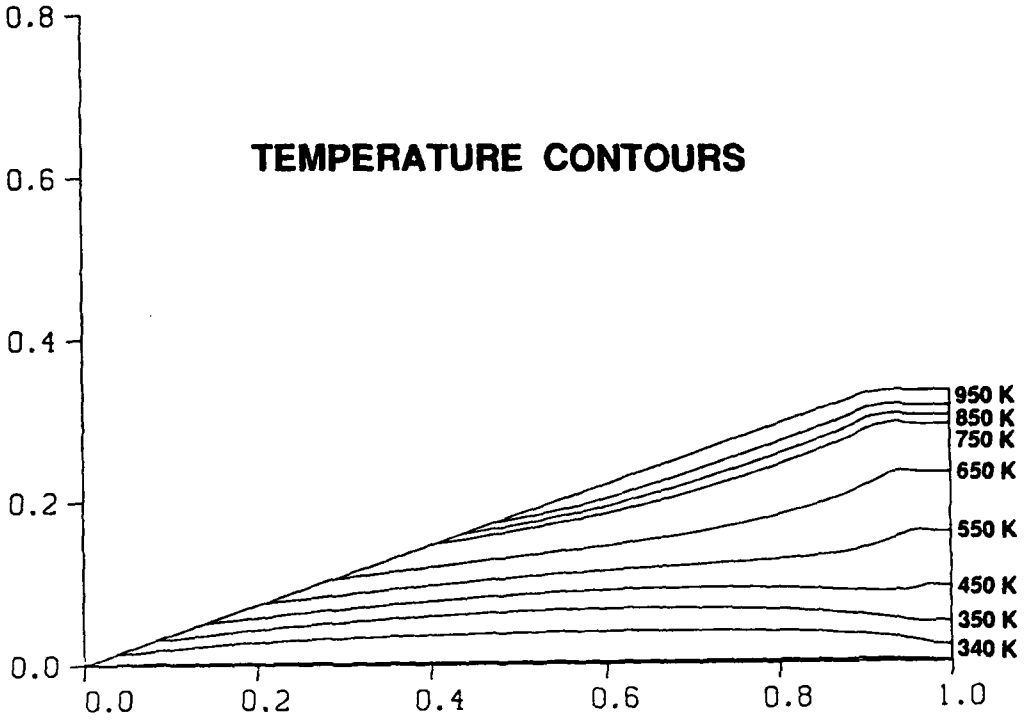

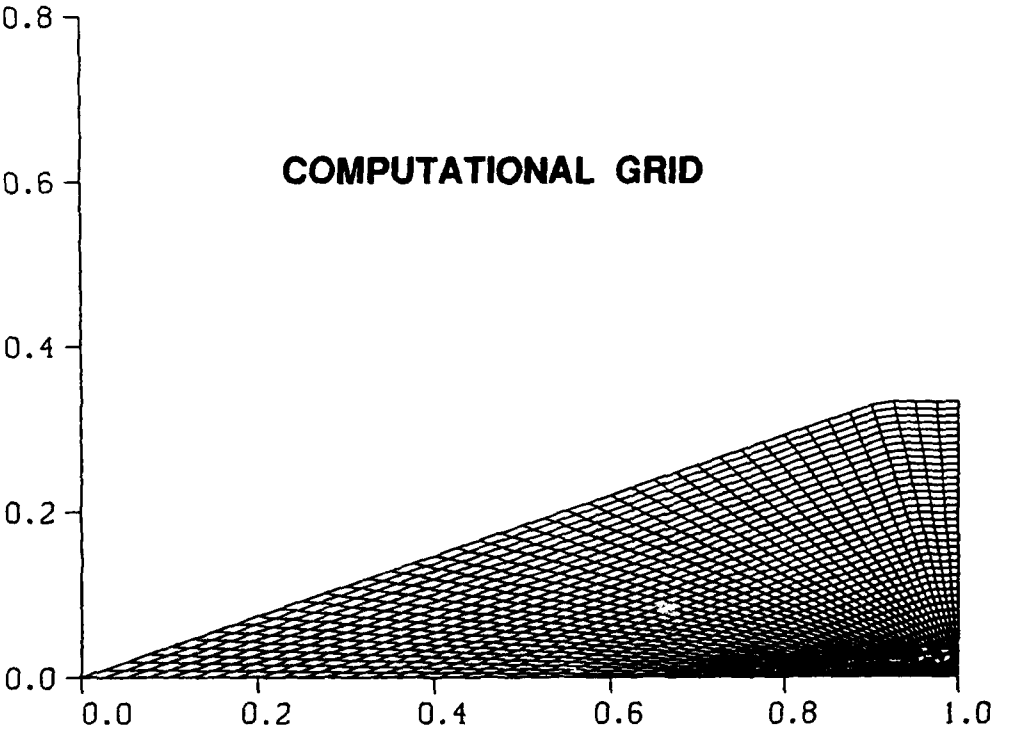

Figure 7. Full 3D fin modeling, Time = 1.0 second

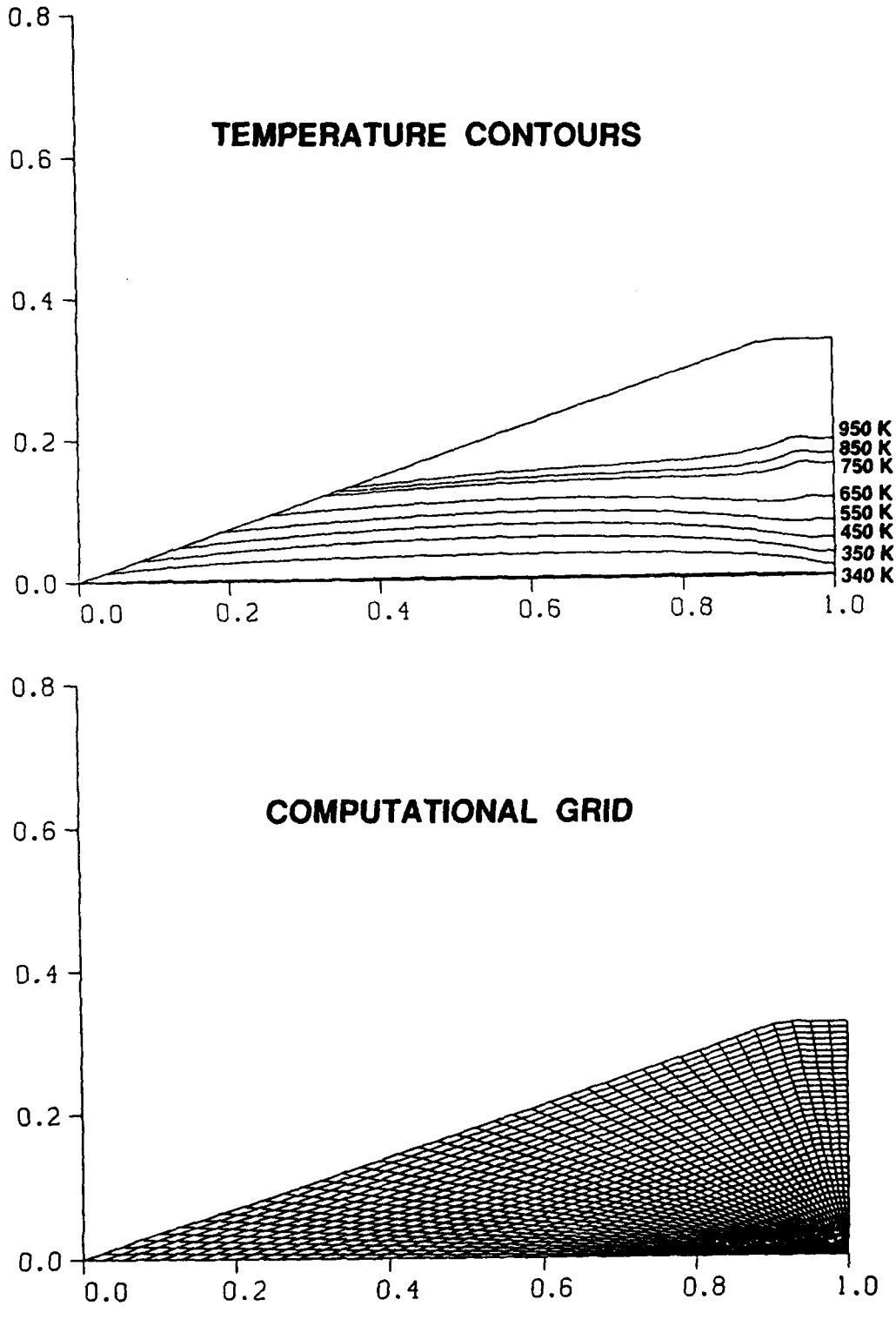

Figure 8. Full 3D fin modeling, Time = 2.0 seconds

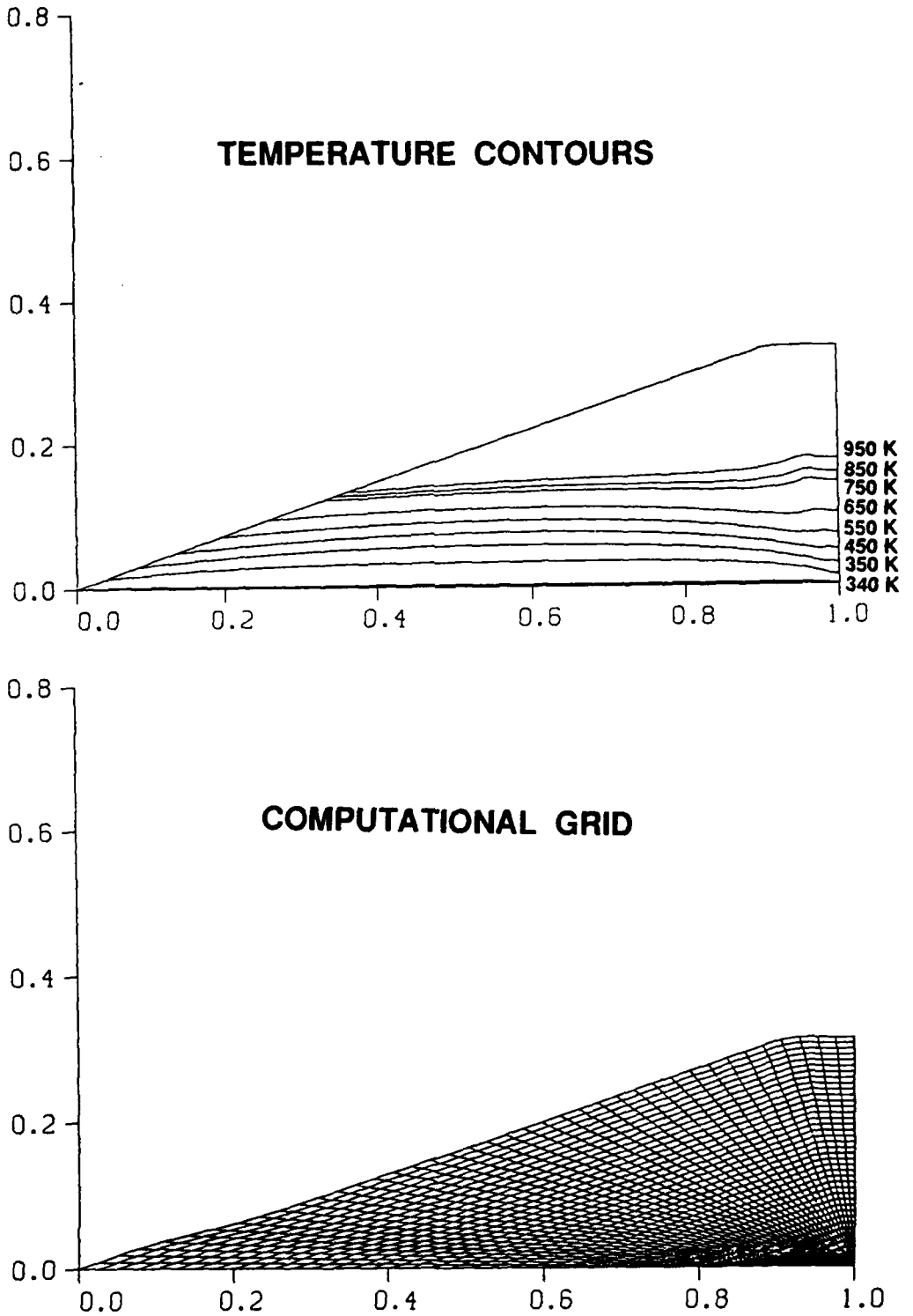

Figure 9. Full 3D fin modeling, Time = 3.0 seconds

INTENTIONALLY LEFT BLANK.

References

1. Sturek, W.B., Kayser, L.D. and P. Weinacht, "Computational Study of Swept-Fin Aerodynamic Heating for the 105mm M774," ARBRL-MR-03315, US Army Ballistic Research Laboratory, Aberdeen Proving Ground, Maryland, October 1983. (AD A134992)

2. Strawn, R.C. and Kobayashi, W.S., "Aerodynamic Heating Computations for Projectiles - Vol. II: Swept Wing Calculations using the Planar Version of the ABRES Shape Change Code (PLNRASCC)," ARBRL-CR-00528, US Army Ballistic Research Laboratory, Aberdeen Proving Ground, Maryland, June 1984. (AD A143253)

3. Dwyer, H.A. "Calculation of Low Mach Number Reacting Flows," AIAA Journal, Vol. 28, No. 1, January 1990, pp 98-105.

4. Brandon, F.J., unpublished range data, private communications, US Army Ballistic Research Laboratory, Aberdeen Proving Ground, Maryland, November 1989.

INTENTIONALLY LEFT BLANK.

LIST OF SYMBOLS

$\vec{A}$	local surface area
$\vec{A}'$	non-dimensional surface area, $\vec{A}'/L^2$
c_v	specific heat
e	internal energy $= c_v T$
h_{bl}	local boundary-layer convective heat transfer coefficient
h_{loc}	local value of h_{bl}
h_{max}	h_{bl} at the fin leading edge
h_{min}	h_{bl} on the fin flat surface
h_{ml}	local boundary-layer convective heat transfer coefficient for melting surface
k	thermal conductivity of the fin
k_f	thermal conductivity of the alumina coating
L	reference length, fin chord at root
L_h	latent heat of the melting fin material
$\vec{n}$	unit normal vector
$\vec{q}$	conduction heat flux $= -k\nabla T$, outward direction positive
$\vec{q}_{adj}$	heat flux per unit area to adjacent control volumes
$\vec{q}_{bl}$	heat flux through viscous boundary layer
$\vec{q}_f$	heat flux through coating
q_{sur}	heat flux into the fin
T	temperature
T'	non-dimensional temperature, T/T_{ref}
T_{melt}	melt temperature of the fin
T_o	local adiabatic wall temperature
T_{ref}	arbitrary reference temperature, 2000 K
T_s	surface temperature of the aluminum
V	volume
V'	non-dimensional volume, V/L^3
$\vec{V}_b$	velocities of the grid boundaries, $\vec{V}_b$, positive outward
$\vec{V}_b'$	non-dimensional velocity at grid boundary $\vec{V}_b/L/\alpha$
x_{loc}	distance from fin leading edge

Greek Symbols

α	thermal diffursivity, $k/\rho c$
Δc	increment along fin chord where the value of h_{bl} changes from h_{max} to h_{min}
Δx_f	local thickness of the alumina coating
Λ	fin leading edge sweep angle
ρ	density
τ	non-dimensional time, $t\alpha/L^2$

INTENTIONALLY LEFT BLANK.

APPENDIX A: CODE IMPLEMENTATION ON THE BRL CRAY2

The heat transfer code is currently run and maintained on the Cray 2 Supercomputer at BRL, but this can also be run on the Cray X-MP/48 Supercomputers with no changes necessary to the code. The code is maintained using a Unix Makefile. This recompiles and links only the code sections which have been changed since the last time the program was complied and linked. This is the fastest, easiest, most efficient way to accurately maintain the source code. The Makefile creates the executable code which is then run on the Cray. A copy of this Makefile follows:

```
#echo
#echo
#echo
#echo  !!!!!!!!!!!!!!!!!!!!!!!!!!!!!!!!!!!!!!!!!!!!!!!!!!!!!!!!!!!!!!!!!!!!!!!!!!!!!!!!!!!!!!!!!!!!!!!!!
#echo
#echo  The Subroutines Are Being Compiled With Optimization Turned On
#echo
#echo  !!!!!!!!!!!!!!!!!!!!!!!!!!!!!!!!!!!!!!!!!!!!!!!!!!!!!!!!!!!!!!!!!!!!!!!!!!!!!!!!!!!!!!!!!!!!!!!!!
#echo
#
#
#
#geom.h phyvar.h solver2.h hbc.h
#include/geom.h include/phyvar.h include/solver2.h include/hbc.h
#include/geom.h include/phyvar.h include/solver2.h include/hbc.h
#
#

3dfin:  nmang3f1.o nmang3f2.o nequa3f.o ninterp.o nmath3f.o
        segldr -o 3dfin nequa3f.o nmang3f1.o nmang3f2.o nmath3f.o interp.o

#
#

        echo
        echo
        echo  '            LINKING PROGRAM'
        echo
        echo
        echo
        echo  '            OPTIMIZATION ON'
        echo
        echo  '            DONE'


#
```

```
nmang3f1.o: mang3f1.f include/geom.h include/phyvar.h
include/solver2.h include/hbc.h
        echo '          COMPILING MANG3F1.F'
        /lib/cpp -P mang3f1.f>nmang3f1.f
        cft77 nmang3f1.f

#
#
#

nmang3f2.o: mang3f2.f include/geom.h include/phyvar.h
include/solver2.h include/hbc.h
        echo '          COMPILING MANG3F2.F'
        /lib/cpp -P mang3f2.f>nmang3f2.f
        cft77 nmang3f2.f

#
#
#

nequa3f.o: equa3f.f include/geom.h include/phyvar.h
include/solver2.h include/hbc.h
        echo '          COMPILING EQUA3F.F'
        /lib/cpp -P equa3f.f>nequa3f.f
        cft77 nequa3f.f

#
#
#

nmath3f.o: math3f.f include/geom.h include/phyvar.h
include/solver2.h include/hbc.h
        echo '          COMPILING MATH3F.F'
        /lib/cpp -P math3f.f>nmath3f.f
        cft77 nmath3f.f

#
#
#

ninterp.o: interp.f include/geom.h include/phyvar.h
include/solver2.h include/hbc.h
        echo '          COMPILING INTERP.F'
        /lib/cpp -P interp.f>ninterp.f
        cft77 ninterp.f
```

Everything in the Makefile which is preceded with a "#" is a comment. The following line from the Makefile sets up the dependencies for the executable code.

```
3dfin:  nmang3f1.o nmang3f2.o nequa3f.o ninterp.o nmath3f.o
        segldr -o 3dfin nequa3f.o nmang3f1.o nmang3f2.o nmathfa.o ninterp.o
```

What this means is, the executable code "3dfin" depends on the five object code files which follow it. They are linked using the Cray 2 linker "segldr." All through the Makefile you see lines which are "indented" from the first column. These MUST be indented with a "tab" character, NOT by spaces. This is a restriction of the Makefile, not the operating system.

The following line sets up the dependencies of the "nmang3f1" object code. This line means the object code depends on the fortran source code file and the four include files which are located in a subdirectory called "include."

```
nmang3f1.o: mang3f1.f include/geom.h include/phyvar.h
include/solver2.h include/hbc.h
        echo '          COMPILING MANG3F1.F'
        /lib/cpp -P mang3f1.f>nmang3f1.f
        cft77 nmang3f1.f
```

Due to the length of the code and the numerous "common" statements, the code is set up to use "include" statements. This allows you to make a change in the ".h" file and the Makefile then changes it throughout the entire code rather than having to make the changes all yourself. However, the include statement is not part of standard fortran, so the code is first run through the C-Preprocessor which actually brings in the common blocks stored in the ".h" files. This is done with the "/lib/cpp -P....." line of the Makefile. The output of this preprocessor is redirected to the file "nxxxxx.f " which is the fortran source code with the common blocks replacing the include statements.

To use the include statements, you must have the line:

```
#include"include/xxxx.h"
```

in your fortran code, where "xxxx.h" is the name of the file you want included,and it is located in a subdirectory called "include." This line goes in the fortran code in the place you want the ".h" file to be inserted, and it must start in the FIRST column, not the seventh like your fortran code does.

Due to the length of time necessary for some runs of the code to complete, it is submitted to the batch queues of the Cray. This also protects the run from an unexpected system crash since the code's point of execution is quickly saved if the system crashes, and its execution continues at that point when the system is brought back up. Running the code in this way also frees up your terminal for other work while it is running. To submit the code for execution, a short JCL file is created which contains the path to the executable

code and any input data files. The JCL file also contains the name of the queue in which to run the code, and the maximum amount of CPU time to allocate to it. There is also a line in the JCL file to start and stop timing statistics. This makes it easier to determine if you can run the code in a faster queue the next time you run it since the queues are based on the amount of CPU time required, and the amount of memory required. An example of the JCL file follows:

```
# QSUB-q crayque     # submit job to the pipe queue
# QSUB-eo            # standard error goes to standard out
# QSUB-lm 1mw        # establish per-process memory size limit
# QSUB-lM 1mw        # establish per-request memory size limit
# QSUB-lt 3000       # establish per-process cpu time limit (seconds)
# QSUB-lT 3000       # establish per-request cpu time limit (seconds)
# QSUB               # end of QSUB parameters


cd /lfd/sb/eferry/Q3F
3dfin < inp
```

The first line of the JCL file sends the job to the queue "crayque." This is a "pipe" queue, which means, there is a series of six queues that the job may run in. The system looks at the requirements of the job and compares this to the limitations of the six queues, and the job gets submitted into the most appropriate queue. The next line combines the standard error file and the standard output file into one - the standard output file. The next two lines set up the memory requirements for the code. Here, the requirements are 1 mega-word. The fifth and sixth lines in this JCL file set the maximum time limit of execution to 3000 seconds CPU time. The next line supplies the path to the code to be run. The "3dfin" is the actual executable code, and the "< inp" redirects Unix standard input from the file "inp" rather than from the keyboard on your terminal.

As the code is executing, the real time of flight is being calculated at each time step. When this time just exceeds predetermined values, a data file is written out with the fin's grid geometry and the temperature at all the grid points. This file is then transferred to an Iris Silicon Graphics work station where it can be graphically displayed. The code which creates this display is written in fortran and calls on the Iris' extensive graphics library to visually display the current state of the fin. This can be done in one of two ways. One way is to view single data files at a time. This is helpful to make sure the code appears to be running correctly before you let it go to its completion. It is also useful for creating hard copies of the fin on a Tektronix 4692 color inkjet printer. The other way this display can be seen is to read in all the data files at one time and display them in rapid succession. This allows the viewer to get a feel as to how the heat is transferring through the fin.

The second method of display uses a mode called "double buffered mode" to make the successive images appear on the screen more fluidly. In this mode, as you are viewing one image, the next image is being drawn in a buffer "behind" it. This image is invisible to you until the buffers are swapped. When the buffers are swapped, the grid you were viewing gets pushed to the back and is redrawn to the next image you will see and the

grid you just drew is presented in front of you. This method is very useful to more easily see how the fin changes from one time to the next, especially if the quasi-3d melting code is being run so you can actually see the fin melt away at each time step.

There is also a program on the Iris workstation for viewing temperature contours. This program was written by Harry Dwyer using GSS on an IBM compatible PC, and was ported to the Iris by Earl N. Ferry, Jr. The program uses a method of shading on the Iris known as Gouraud shading to achieve smooth contours. This is accomplished by creating a color map and interpolating the temperatures of the grid onto the indices of the color map. These indices are then used as color shades for the fill routine. This method of coloring the grid creates a smooth blend of colors for the different temperatures.

There are also a few short programs using DISSPLA written on the Cray 2 which allow you to get fast visual results of the grid. This is also helpful to make sure the code is executing properly before you ship the data files over to the Iris work stations.

INTENTIONALLY LEFT BLANK.

No of Copies	Organization
1	Office of the Secretary of Defense OUSD(A) Director, Live Fire Testing ATTN: James F. O'Bryon Washington, DC 20301-3110
2	Administrator Defense Technical Info Center ATTN: DTIC-DDA Cameron Station Alexandria, VA 22304-6145
1	HQDA (SARD-TR) WASH DC 20310-0001
1	Commander US Army Materiel Command ATTN: AMCDRA-ST 5001 Eisenhower Avenue Alexandria, VA 22333-0001
1	Commander US Army Laboratory Command ATTN: AMSLC-DL Adelphi, MD 20783-1145
2	Commander US Army, ARDEC ATTN: SMCAR-IMI-I Picatinny Arsenal, NJ 07806-5000
2	Commander US Army, ARDEC ATTN: SMCAR-TDC Picatinny Arsenal, NJ 07806-5000
1	Director Benet Weapons Laboratory US Army, ARDEC ATTN: SMCAR-CCB-TL Watervliet, NY 12189-4050
1	Commander US Army Armament, Munitions and Chemical Command ATTN: SMCAR-ESP-L Rock Island, IL 61299-5000
1	Commander US Army Aviation Systems Command ATTN: AMSAV-DACL 4300 Goodfellow Blvd. St. Louis, MO 63120-1798

No of Copies	Organization
1	Director US Army Aviation Research and Technology Activity ATTN: SAVRT-R (Library) M/S 219-3 Ames Research Center Moffett Field, CA 94035-1000
1	Commander US Army Missile Command ATTN: AMSMI-RD-CS-R (DOC) Redstone Arsenal, AL 35898-5010
1	Commander US Army Tank-Automotive Command ATTN: AMSTA-TSL (Technical Library) Warren, MI 48397-5000
1	Director US Army TRADOC Analysis Command ATTN: ATAA-SL White Sands Missile Range, NM 88002-5502
(Class. only) 1	Commandant US Army Infantry School ATTN: ATSH-CD (Security Mgr.) Fort Benning, GA 31905-5660
(Unclass. only) 1	Commandant US Army Infantry School ATTN: ATSH-CD-CSO-OR Fort Benning, GA 31905-5660
1	Air Force Armament Laboratory ATTN: AFATL/DLODL Eglin AFB, FL 32542-5000
	Aberdeen Proving Ground
2	Dir, USAMSAA ATTN: AMXSY-D AMXSY-MP, H. Cohen
1	Cdr, USATECOM ATTN: AMSTE-TD
3	Cdr, CRDEC, AMCCOM ATTN: SMCCR-RSP-A SMCCR-MU SMCCR-MSI
1	Dir, VLAMO ATTN: AMSLC-VL-D

No. of Copies	Organization
4	Commander US Army, ARDEC ATTN: SMCAR-AET-A, Kline Chung Kahn Hudgins Picatinny Arsenal, NJ 07806-5000
4	Commander US Army, ARDEC ATTN: SMCAR-CCL-CA, Hirlinger O'Neill Miller SMCAR-CCL-EM(B65N), Rao Yalamanchili Picatinny Arsenal, NJ 07806-5000
1	Commander US Army, ARDEC ATTN: SMCAR-FSP-A(1)(Bischer) Picatinny Arsenal, NJ 07806-5000
2	Commander Naval Surface Warfare Center ATTN: Code DK20, Clare Moore Dahlgren, VA 22448-5000
2	Director Sandia National Laboratories ATTN: Dr. W. Oberkampf Dr. F. Blottner Division 1636 P.O. Box 5800 Albuquerque, NM 87185
1	Massachusetts Institute of Technology ATTN: Tech Library 77 Massachusetts Avenue Cambridge, MA 02139
2	Commander David W. Taylor Naval Ship ATTN: Dr. S. de los Santos Mr. Stanley Gottlieb Bethesda, MD 20084-5000

No. of Copies	Organization
1	Virginia Polytechnic Institute and State University P.O. Box 50 Blacksburg, VA 24061
1	Commandant USAFAS ATTN: ATSF-TSM-CN Fort Sill, OK 73503-5600
2	Ford Aerospace and Communications Corporation Aeronautics Division ATTN: Charles White Bud Blair Ford Road Newpoint Beach, CA 92658
2	Honeywell, Inc. ATTN: Mark W. Swensen Richard J. Buretta Mail Station MN48-3700 7225 Northland Drive Brooklyn Park, MN 55428
1	NASA, Langley Research Center Transonic Aerodynamics Division ATTN: Dr. Michael J. Hemsch Hampton, VA 23665
1	Applied Technology Associates ATTN: Mr. R.J. Cavalleri P.O. Box 19434 Orlando, FL 32814
1	Arrow Technology Associates ATTN: Robert Whyte P.O. Box 4218 Burlington, VT 05491-0042
2	United States Military Academy Department of Civil and Mechanical Engineering ATTN: LTC Andrew L. Dull CPT Kent Eisele West Point, NY 10996

USER EVALUATION SHEET/CHANGE OF ADDRESS

This Laboratory undertakes a continuing effort to improve the quality of the reports it publishes. Your comments/answers to the items/questions below will aid us in our efforts.

1. BRL Report Number BRL-MR-3852 Date of Report August 1990

2. Date Report Received _____

3. Does this report satisfy a need? (Comment on purpose, related project, or other area of interest for which the report will be used.) _____

4. Specifically, how is the report being used? (Information source, design data, procedure, source of ideas, etc.) _____

5. Has the information in this report led to any quantitative savings as far as man-hours or dollars saved, operating costs avoided, or efficiencies achieved, etc? If so, please elaborate. _____

6. General Comments. What do you think should be changed to improve future reports? (Indicate changes to organization, technical content, format, etc.) _____

CURRENT ADDRESS

Name

Organization

Address

City, State, Zip Code

7. If indicating a Change of Address or Address Correction, please provide the New or Correct Address in Block 6 above and the Old or Incorrect address below.

OLD ADDRESS

Name

Organization

Address

City, State, Zip Code

(Remove this sheet, fold as indicated, staple or tape closed, and mail.)

----------FOLD HERE----------

DEPARTMENT OF THE ARMY
Director
U.S. Army Ballistic Research Laboratory
ATTN: SLCBR-DD-T
Aberdeen Proving Ground, MD 21[illegible]-5066
OFFICIAL BUSINESS

NO POSTAGE
NECESSARY
IF MAILED
IN THE
UNITED STATES

BUSINESS REPLY MAIL
FIRST CLASS PERMIT No 0001, APG, MD

POSTAGE WILL BE PAID BY ADDRESSEE

Director
U.S. Army Ballistic Research Laboratory
ATTN: SLCBR-DD-T
Aberdeen Proving Ground, MD 21005-9989

----------FOLD HERE----------